AFRL-ML-WP-TP-2007-503

ACCURATE EVALUATION NONLINEAR ABSORPTION COEFFICIENTS FOR LIGHT PROPAGATION IN InAs, InSb, AND HgCdTe ALLOYS (Preprint)

Srini Krishnamurthy, Zhi Gang Yu, Leo Gonzalez, and Shekhar Guha

Agile IR Limiters, Exploratory Development
Hardened Materials Branch
Survivability and Sensor Materials Division

JANUARY 2007

AIR FORCE RESEARCH LABORATORY
MATERIALS AND MANUFACTURING DIRECTORATE
WRIGHT-PATTERSON AIR FORCE BASE, OH 45433-7750
AIR FORCE MATERIEL COMMAND
UNITED STATES AIR FORCE

NOTICE

Using Government drawings, specifications, or other data included in this document for any purpose other than Government procurement does not in any way obligate the U.S. Government. The fact that the Government formulated or supplied the drawings, specifications, or other data does not license the holder or any other person or corporation; or convey any rights or permission to manufacture, use, or sell any patented invention that may relate to them.

This report was cleared for public release by the Air Force Research Laboratory Wright Site (AFRL/WS) Public Affairs Office (PAO) and is releasable to the National Technical Information Service (NTIS). It will be available to the general public, including foreign nationals.

THIS TECHNICAL REPORT IS APPROVED FOR PUBLICATION.

*//signature//

SHEKHAR GUHA, Ph.D.
Agile IR Limiters
Exploratory Development
Hardened Materials Branch

//signature//

MARK S. FORTE, Acting Chief
Hardened Materials Branch
Survivability and Sensor Materials Division

//signature//

TIM J. SCHUMACHER, Chief
Survivability and Sensor Materials Division
Materials and Manufacturing Directorate

This report is published in the interest of scientific and technical information exchange and its publication does not constitute the Government's approval or disapproval of its ideas or findings.

*Disseminated copies will show "//signature//" stamped or typed above the signature blocks.

REPORT DOCUMENTATION PAGE

Form Approved
OMB No. 0704-0188

1. REPORT DATE *(DD-MM-YY)*	2. REPORT TYPE	3. DATES COVERED *(From - To)*
January 2007	Journal Article Preprint	

4. TITLE AND SUBTITLE

ACCURATE EVALUATION NONLINEAR ABSORPTION COEFFICIENTS FOR LIGHT PROPAGATION IN InAs, InSb, AND HgCdTe ALLOYS (Preprint)

5a. CONTRACT NUMBER
IN-HOUSE

5b. GRANT NUMBER

5c. PROGRAM ELEMENT NUMBER
62102F

6. AUTHOR(S)

Srini Krishnamurthy and Zhi Gang Yu (SRI International)
Leo Gonzalez and Shekhar Guha (Agile IR Limiters, Exploratory Development)

5d. PROJECT NUMBER
4348

5e. TASK NUMBER
RG

5f. WORK UNIT NUMBER
M03R1000

7. PERFORMING ORGANIZATION NAME(S) AND ADDRESS(ES)

Agile IR Limiters, Exploratory Development
Hardened Materials Branch, Survivability and Sensor Materials Division
Materials and Manufacturing Directorate, Air Force Research Laboratory
Wright-Patterson Air Force Base, OH 45433-7750
Air Force Materiel Command, United States Air Force

SRI International
333 Ravenswood Ave.
Menlo Park, CA 94025

8. PERFORMING ORGANIZATION REPORT NUMBER
AFRL-ML-WP-TP-2007-503

9. SPONSORING/MONITORING AGENCY NAME(S) AND ADDRESS(ES)
Air Force Research Laboratory
Materials and Manufacturing Directorate
Wright-Patterson Air Force Base, OH 45433-7750
Air Force Materiel Command
United States Air Force

10. SPONSORING/MONITORING AGENCY ACRONYM(S)
AFRL/MLPJ

11. SPONSORING/MONITORING AGENCY REPORT NUMBER(S)
AFRL-ML-WP-TP-2007-503

12. DISTRIBUTION/AVAILABILITY STATEMENT
Approved for public release; distribution unlimited.

13. SUPPLEMENTARY NOTES
The U.S. Government is joint author of this work and has the right to use, modify, reproduce, release, perform, display, or disclose the work. PAO case number AFRL/WS 06-2656, 08 November 2006. Submitted to the Journal of Applied Physics.

14. ABSTRACT

We present a full-bandstructure calculation of temperature- and wavelength-dependent two-photon absorption (TPA) coefficients and free-carrier absorption (FCA) cross sections in InAs, InSb, $Hg_{1-x}Cd_xTe$ alloys. Although the wavelength dependence of the TPA coefficients agrees well with widely used analytical expression, our calculated values are smaller by a factor of 1.2 to 2.5. In addition, the TPA coefficient depends sensitively on the photoexcited carrier density in small gap materials. The FCA is found to be due predominantly to holes. The FCA cross section is independent of the carrier density, but strongly dependent on the temperature. The calculated coefficients and lifetimes are fitted to closed-form expressions and used in solving the rate equations to obtain the transmitted pump and probe intensities as functions of incident intensity and sample thickness. The calculated pump transmission and time-dependent probe transmission in InAs agree very well with the measured values.

15. SUBJECT TERMS
Two-photon absorption(TPA), free-carrier absorption(FCA), Bandstructure

16. SECURITY CLASSIFICATION OF:			17. LIMITATION OF ABSTRACT:	18. NUMBER OF PAGES	19a. NAME OF RESPONSIBLE PERSON (Monitor)
a. REPORT	b. ABSTRACT	c. THIS PAGE			Dr. Shekhar Guha
Unclassified	Unclassified	Unclassified	SAR	36	19b. TELEPHONE NUMBER *(Include Area Code)* (937) 255-4588

Standard Form 298 (Rev. 8-98)
Prescribed by ANSI Std. Z39-18

Accurate evaluation nonlinear absorption coefficients for light propagation in InAs, InSb and HgCdTe alloys

Srini Krishnamurthy, Zhi Gang Yu
SRI International, 333 Ravenswood Avenue, Menlo Park, CA 94025
Leo Gonzalez[(a)] and Shekhar Guha[(b)]
(a) Air Force Research Laboratory, Materials and Manufacturing Directorate, General Dynamics Information Technology, Dayton, OH, 45431
(b) Air Force Research Laboratory, Materials and Manufacturing Directorate, Wright-Patterson Air Force Base, Ohio, 45433

ABSTRACT

We present a full-bandstructure calculation of temperature- and wavelength-dependent two-photon absorption (TPA) coefficients and free-carrier absorption (FCA) cross sections in InAs, InSb, $Hg_{1-x}Cd_xTe$ alloys. Although the wavelength dependence of the TPA coefficients agrees well with widely used analytical expression, our calculated values are smaller by a factor of 1.2 to 2.5. In addition, the TPA coefficient depends sensitively on the photoexcited carrier density in small gap materials. The FCA is found to be due predominantly to holes. The FCA cross section is independent of the carrier density, but strongly dependent on the temperature. The calculated coefficients and lifetimes are fitted to closed-form expressions and used in solving the rate equations to obtain the transmitted pump and probe intensities as functions of incident intensity and sample thickness. The calculated pump transmission and time-dependent probe transmission in InAs agree very well with the measured values.

INTRODUCTION

The nonlinear optical absorption and refraction properties affect the propagation of high intensity light through transparent materials.[1,2] Several physical mechanisms including two-photon absorption, free- carrier absorption, thermal and free carrier refraction are responsible for nonlinear properties.[3-6] Both theory and experiments are constantly being improved to accurately evaluate nonlinear absorption and refraction coefficients.[7-22] When the energy of high-intensity incident photons is more than a half of the band gap of the semiconductor, the electrons in the valence band (VB) absorb two photons to reach unoccupied states in the conduction band (CB). Then the photoexcited electrons and holes further absorb a photon with or without assistance of a phonon, causing further reduction in intensity as the light travels through the material. Since the two- photon absorption (TPA) plays a vital role to initiate on the nonlinearity in the material, a number of studies have been undertaken to accurately evaluate the TPA coefficient. However, the extraction of TPA values from experiments often depended on the ability to control other factors that simultaneously affect the nonlinear absorption. Consequently, the extracted values varied substantially.[7-10,15,18-21] On the theoretical side, the Wherrett's expression[12] with nonparabolic correction[11] is used widely. Later it was modified and the interaction matrix element was parameterized based on the **k**.**p** models to successfully predict the trends in various semiconductors.[14-17] This expression has served an excellent role in providing qualitative trends and giving approximate values for the TPA coefficients in understanding light propagation. However, an accurate evaluation, with full band structures and matrix elements included, of TPA coefficient made recently[22,23] has revealed that the calculated values differ substantially from those given by the simple analytical formula.

Light propagation is further affected by free carrier absorption (FCA), in which the TPA generated photoexcited carriers absorb photons. The cross section of the free carrier absorption, defined as the ratio of free carrier absorption coefficient to the free carrier density, is in general assumed to be a constant in light propagation studies.[3-6] However, in our detailed calculations we find that the cross section is strongly dependent on wavelength and temperature. We have carried out these calculations with full band

structures for InSb, InAs, and $Hg_{1-x}Cd_xTe$ alloys. The room-temperature band gap of InAs and InSb are 0.35 eV and 0.175 respectively.

In this paper, we first provide a brief description of the bandstructures, the quasi Fermi energies and nonlinear absorption coefficients (TPA and FCA). The wavelength and carrier density dependence of the TPA and FCA coefficients in InAs, InSb, and HgCdTe alloys are reported. The calculated values of TPA and FCA in InSb, InAs, and HgCdTe alloys (with x=0.238 and x=0.344) are also fitted to simple analytical form so it can be used easily in light propagation modeling.[3-6,24] These values are used in obtaining a solution to rate equation that describes the light propagation through InAs. The results are compared with experiments.

THEORY

Second-order perturbation theory is used to calculate the TPA and FCA coefficients[22] and Auger and radiative recombination lifetimes.[25] The dipole matrix elements, required to study light interaction with matter, and the scattering matrix elements, required in lifetime calculations, are calculated from underlying bandstructures. Care is taken to describe the occupancy of initial and final states with appropriate Fermi-Dirac distributions and to include accurate sum over crystal wave vectors spanning the entire Brillouin zone (BZ).

Band Structures

The calculations reported here are based on a hybrid pseudopotential tight-binding Hamiltonian.[26] In this formalism, the tight-binding Hamiltonian contains two parts. The dominant part is derived from the empirical pseudopotential and includes all long-range interactions. A short-range empirical Hamiltonian is added to fine-tune the calculated band structure to agree with the measured energy gaps and effective masses at various symmetry points in the BZ. In the sp^3 basis, with the spin-orbit coupling included, the Hamiltonian takes 16 ×16 matrix form. In the case of alloys, we find that the correction to bands from the alloy disorder is small near the band edge, and hence the virtual crystal approximation can be used to obtain the alloy band structures. The resulting Hamiltonian matrix is diagonalized to yield the eigenvalues (energies) and eigenvectors (wave functions).

Since a high intensity light absorbed in a material can raise the material temperature substantially above room temperature, we are interested in using bandstructures over a wide range of temperatures from 77 K up to ~500K. Although the temperature (T) dependence of the matrix elements can be included[27] for the calculation of the band structure, those calculations are extremely time-consuming, particularly when the integration over the full BZ is required in lifetime calculations. Here, as an alternative, the effect of T on the $Hg_{1-x}Cd_xTe$ alloy band structure is included indirectly as follows. First, for a given T and Cd concentration x, the band gap E_g in eV is determined from the widely used relationship,[28] $-0.302 + 1.93x + 5.35\ 10^{-4}\ (1-2x)*T - 0.81x^2 + 0.832x^3$. We then adjust the value of **x** in our zero-temperature Hamiltonian to x' to get the band gap of E_g. The zero-temperature Hamiltonian with the value of x' is then used in further calculations. In the case of InAs[29] and InSb[30] compounds, the parameters of the short-range empirical Hamiltonian are adjusted at each temperature to yield the band gap in eV given by $0.415 - 2.76\times10^{-4}\ T^2/(T+83)$ and $0.24 - 6\times10^{-4}\ T^2/(T+500)$ respectively. The calculated band gap energy as a function of T is shown by dashed line in Figure 1 (a) InAs, (b) $Hg_{0.66}Cd_{0.34}Te$, (c) InSb, and (d) $Hg_{0.76}Cd_{0.24}Te$. We see that the band gap decreases with T in InAs and InSb, but increases in HgCdTe alloys.

Fermi Level

The study of electron-photon interaction requires the knowledge of the electron density and its distribution. The Boltzmann distribution is often used. However, at high temperatures and for small gap materials, the bands are nearly or fully degenerate and the Fermi-Dirac (FD) distribution is required in the functional form,

$$f(E,E_f) = \left[1 + e^{(E-E_f)/k_BT}\right]^{-1}$$

where k_B is the Boltzmann constant. The equilibrium Fermi level (FL) or Fermi energy E_f is obtained from the charge neutrality condition that the total positive charges (the sum of hole density p_0 and ionized donors N_D^+) equals the total negative charges (the sum of electron density n_0 and ionized acceptors N_A^-).[31] The quantities n_0, p_0, N_D^+ and N_A^- in turn depend on the Fermi energy:

$$N_D^+ = N_D\left[1+ge^{(E_f-E_D)/k_BT}\right]^{-1}; \qquad N_A^- = N_A\left[1+ge^{(E_A-E_F)/k_BT}\right]^{-1}$$

$$n_0 = 2\int_{E_c}^{\infty}\rho_c(E-E_c)f(E,E_f)dE; \qquad p_0 = 2\int_{-\infty}^{E_v}\rho_v(E-E_v)f(E,E_f)dE;$$

$$\rho_{c,v} = \frac{1}{\Omega}\sum_{\mathbf{k}}\delta\left(E_{c,v}^{\mathbf{k}}-E\right)$$

Under high-intensity of light illumination, very large photoexcited electron density (Δn) and hole density (Δp) are created. Although $\Delta n = \Delta p$, they can be far above their intrinsic values of n_0 and p_0. Consequently, the TPA, FCA coefficients and lifetime calculations have to be carried out not only under degenerate conditions, but also under nonequilibrium condition in which the electrons in the CB and the holes in the VB have different Fermi energies. These quasi Fermi energy for electrons (E_f^c) and holes (E_f^v) are determined from the following conditions:

$$n_0 + \Delta n = 2\int_{E_c}^{\infty}\rho_c(E-E_c)f(E,E_f^c)dE$$

$$p_0 + \Delta p = 2\int_{-\infty}^{Ev}\rho_c(E-E_v)f(E,E_f^v)dE$$

where E_c and E_v are the band energies at CB minimum and and VB maximum respectively..

In Figure 1, we have shown the calculated electron (thin solid line) and hole (thick solid line) Fermi energies as functions of the lattice temperature and excited carrier density in (a) InAs, (b) $Hg_{0.66}Cd_{0.34}Te$, (c) InSb, and (d) $Hg_{0.76}Cd_{0.24}Te$. When the excited electron (Δn) and hole (Δp) densities are zero, we obtain the intrinsic Fermi energy, shown by dotted line. All energies are measured with respect to the top of the VB at that temperature. At low temperature, the intrinsic FL is near mid-gap and moves closer to the CB edge (shown by dashed line) with an increase in T. In the case of InSb, we see that the FL lies above the bottom of the CB at high temperature, making the material fully degenerate. In HgCdTe alloys, the band gap increases with T and hence the intrinsic FL is lies below the CB for all the temperatures considered here. When the photoexcited carrier density ($\Delta n=\Delta p$) is finite and larger than the intrinsic carrier density at that T, the quasi FL for electron and holes are closer to the CB and the VB

respectively. The quasi FLs merge with the intrinsic FL when the intrinsic carrier density is larger than the photoexcited carrier density. The intrinsic carrier density increases with T and decreases with E_g, as seen in Figure 2. Consequently, quasi FLs play major role even in systems with moderate excited densities at low T and in systems with large densities at high T in general. This trend is clearly seen in Figure 1. Recently, the variable Hall studies, in combination with multiple carrier analysis, have demonstrated to be able to a yield accurate measurement of the carrier density in doped samples.[32-34] The carrier densities calculated using our band structures were found to be in excellent agreement with the measurements.[17]

Two-photon absorption

Electrons in the heavy-hole (HH) and light-hole (LH) valence bands absorb two photons to reach the CB states. In the second order perturbation theory, the absorption rate is proportional to the occupation of the initial state in the VB, availability of the final state in the CB, and the dipole matrix element between the VB and CB states at a given crystal momentum. Explicitly, the expression for TPA coefficient β is:

$$\beta = \frac{1}{\pi c}\left(\frac{2\pi e}{m}\right)^4 \frac{1}{(\omega_0 n)^3}\sum_{\alpha\beta\mathbf{k}}\left(1-f(E_\beta^{\mathbf{k}},E_f^{\beta})\right)|M_{\alpha\beta}^{\mathbf{k}}|^2\, f(E_\alpha^{\mathbf{k}},E_f^{\alpha})\delta\left(E_\alpha^{\mathbf{k}}-E_\beta^{\mathbf{k}}+2\hbar\omega_0\right)$$

$$M_{\alpha\beta}^{\mathbf{k}} = \sum_{\beta'}\sum_{jj'}\frac{\langle\phi_\beta^{\mathbf{k}}|\mathbf{e}_{j'}\cdot\mathbf{p}|\phi_{\beta'}^{\mathbf{k}}\rangle\langle\phi_{\beta'}^{\mathbf{k}}|\mathbf{e}_j\cdot\mathbf{p}|\phi_\alpha^{\mathbf{k}}\rangle}{\mathbf{E}_\alpha^{\mathbf{k}}-\mathbf{E}_{\beta'}^{\mathbf{k}}+\hbar\omega_0}$$

where $E_\beta^{\mathbf{k}}(\phi_\beta^{\mathbf{k}})$ is the electron energy (wave function) in the band β at the wave vector **k** in the BZ, *e* and *m* are free electron change and mass, *n* is the real part of the refractive index, **p** is electric dipole vector, $\mathbf{e}_j$ is the polarization of light, and $\hbar\omega_0$ is photon energy. Note that the FD distribution for the electrons, $f(E_\beta^{\mathbf{k}})$ uses appropriate quasi Fermi energy E_f^v and E_f^c depending on whether β denotes a valence or a CB. In the above expression, α and β denote respectively initial and final state in any occupied VB and any unoccupied CB that satisfy the energy conservation condition specified by the δ function. A careful analysis shows that the intermediate state β' can be any of the unoccupied CB

state and one VB state from which the electron excitation begins. The sum over **k** is considered over entire the BZ.

We used full bands to accurately accurate FD distributions, band energy, wave functions, and optical matrix elements, to obtain β as a function of the photon wavelength and T. The calculated β at T=300K and 77K are shown in Figure 3 for (a) InAs, (b) $Hg_{0.66}Cd_{0.34}Te$, (c) InSb, and (d) $Hg_{0.76}Cd_{0.24}Te$. When the wavelength is longer than twice the cutoff wavelength, electrons in the VB cannot reach the CB and β drops to zero. As the wavelength is decreased, more states are available and β increases. However, with further decrease of the wavelength, the energy difference between the initial and final states increases and the rate calculated by the second-order perturbation theory decreases, resulting in a decreased β. This trend is seen in all materials considered here. As the one photon absorption will start to dominate at wavelengths shorter than the cutoff wavelength for the given T, the values of β calculated in that spectral region is not useful. In InAs and InSb, the band gap decreases with T, and consequently β increases. For similar reasons, β in HgCdTe decreases with T. Although the band gaps of InAs and $Hg_{0.66}Cd_{0.34}Te$ at room temperature are equal, β in HgCdTe alloy is considerably higher than in InAs, owing to the difference in the density of states.

For an intrinsic material at a very low temperature, the initial state is full and the final state is empty. However, the occupancy or availability of the states depends on T and the excess carrier density, given by FD distribution as discussed in the previous section. Consequently, the calculated β has a dependence of the photoexcited carrier density as shown in Figure 4 at (a) 300K and (b) 77K. At 300K, the intrinsic carrier density in the large band gap InAs and $Hg_{0.66}Cd_{0.34}Te$ is small and the calculated β shows only slight variation with photoexcited carrier density. However, in the small gap InSb and $Hg_{0.76}Cd_{0.24}Te$, the intrinsic carrier density is large. Additional photoexcited carriers deplete (fill) the near band edge VB (CB) states. Hence, the occupancy (availability) of initial (final) state is different from one (zero), resulting in a decreased β. We see that the calculated β start to decrease for the photoexcited carrier densities in excess of mid 10^{16} cm^{-3}. This effect, commonly known as Moss-Burstein effect, is dominant for small band

gap materials and at low T. The β calculated at 77K shows even stronger carrier density dependence, as shown in Figure 4b.

It is instructive to compare the calculated β to that obtained by most commonly used, but approximate, methods. Quantitatively, the calculated wavelength dependence agrees well with that predicted by the Wherrett's or Van Stryland's expression.[8,11] However, our values calculated, at 4.8 μm and low carrier density, are smaller than those obtained with Van Stryland's expression by a factor of 2.5 for $Hg_{0.66}Cd_{0.34}Te$ and 1.5 for InAs. Similarly, the values calculated at 9.6 μm and low carrier density are smaller by a factor of 2.2 for InSb and 1.2 for $Hg_{0.74}Cd_{0.26}Te$. Although the values calculated by either method are within the experimental accuracy, it is important to note that the newly identified N- and T- dependence will be important in light propagation studies.

The wavelength-dependent calculations of β at low carrier densities are carried out as a function of Cd concentration (x) in $Hg_{1-x}Cd_xTe$ alloys and are shown in Figure 5. The wavelength dependence is similar in all alloys. However, as the value of x increases, the band gap increases and, consequently, β decrease with x. This is clearly seen in Figure 5.

Free carrier absorption

Along with TPA, further absorption light by the photo-generated carriers is possible. When a hole is photo-generated in the heavy-hole (HH) VB, the electrons in the light-hole (LH) band can absorb one photon and get excited to fill that hole. This direct process is normally known as FCA by holes. The associated photo-generated electron in the CB also will absorb a photon. However to satisfy the momentum and energy conservation condition, the photon absorption should accompany a phonon absorption or emission in this indirect process. The free carrier absorption rate calculated from second order perturbation theory is used to obtain FCA coefficient α_f and FCA cross section σ. Although the basic formalism has been described previously,[22] here we provide explicit expressions for two contributions—direct term and indirect term. This helps us separate the contributions from electrons and holes, for an appropriate use in the rate equations. In the direction term, electron from a lower band absorbs a photon and

transfers to a higher band. The initial and final state wave vector remains unchanged, but the final state energy is larger than the initial state energy by $\hbar\omega_0$. We have,

$$\alpha_D = \left(\frac{2\pi e}{m}\right)^2 \left(\frac{1}{n\omega_0 c}\right) \sum_{\alpha\beta\mathbf{k}} f(E_\alpha^{\mathbf{k}}, E_f^\alpha)\left(1 - f(E_\beta^{\mathbf{k}}, E_f^\beta)\right) \left| \sum_j \langle \phi_\beta^{\mathbf{k}} | \mathbf{e}_j \cdot \mathbf{p} | \phi_\alpha^{\mathbf{k}} \rangle \right|^2 \delta\left(E_\beta^{\mathbf{k}} - E_\alpha^{\mathbf{k}} - \hbar\omega_0\right)$$

Since the energy separation between LH and HH bands vary from 0 to several electron volts, this term is non zero for hole-initiated FCA. However, the CBs are separated by energies much larger than the usual phonon energies of interest, and the direct excitation of electrons from the lowest CB to the next highest CB is not possible. Hence, in the expression for α_D, both α and β denote valence bands and the FD function is evaluated with E_f^p. An additional mechanism to supply both momentum and energy is required for CB electrons to participate in the FCA. The most dominant contribution usually arises from longitudinal-phonon (LO) assisted FCA. Using Frohlich Hamiltonian to describe electron-phonon interaction, the absorption coefficient for this indirect process can be written as,

$$\alpha_{ID} = \left(\frac{(2\pi)^3 e^4 \hbar\omega_{LO}}{m^2 \hbar c (\hbar\omega_0)^3}\right)\left(\frac{1}{\kappa_\infty} - \frac{1}{\kappa_0}\right) \sum_{\alpha\beta\mathbf{k}} f(E_\alpha^{\mathbf{k}}, E_f^\alpha) \sum_{\mathbf{q}} \left[1 - f(E_\beta^{\mathbf{k}\pm\mathbf{q}}, E_f^\beta)\right] R_{\alpha\beta}^{\mathbf{kq}} \delta\left[E_\beta^{\mathbf{k}\pm\mathbf{q}} - E_\alpha^{\mathbf{k}} \mp \hbar\omega_{LO} - \hbar\omega_0\right]$$

$$R_{\alpha\beta}^{\mathbf{kq}} = \left(N_{LO} + \frac{1}{2} \mp \frac{1}{2}\right) \left| \langle \phi_\beta^{\mathbf{k}\pm\mathbf{q}} | \frac{e^{i\mathbf{q}.\mathbf{r}}}{q} | \phi_{\beta'}^{\mathbf{k}} \rangle \times \sum_j \left(\langle \phi_{\beta'}^{\mathbf{k}} | \mathbf{e}_j \cdot \mathbf{p} | \phi_\alpha^{\mathbf{k}} \rangle - \langle \phi_{\beta'}^{\mathbf{k}\pm\mathbf{q}} | \mathbf{e}_j \cdot \mathbf{p} | \phi_\alpha^{\mathbf{k}\pm\mathbf{q}} \rangle \right) \right|^2$$

where the $\hbar\omega_{LO}$ and N_{LO} are LO phonon energy and population, κ_0 and κ_∞ are zero and infinite frequency dielectric constant, and ± sign denotes phonon absorption or emission. Other symbols have the same meaning as those defined in the previous section. For the conduction electrons, the initial, intermediate and final states will all be in the lowest CB. However for the holes, the initial and final states can be in either of LH or HH bands. It should be noted that, depending on the bands that contribute to the absorption, the FD functions are evaluated using appropriate quasi Fermi level. The total FCA coefficient, α_f is sum of the two contributions. The FCA cross section for electrons (holes), $\sigma_{e(h)}$ is ratio of the coefficient to the electron (hole) density, $N_{e(h)}$. Simply,

$$\alpha_f = \alpha_D + \alpha_{ID}$$

$$\sigma_{e(h)} = \frac{\alpha_f}{N_{e(h)}}$$

As expected, the calculated rate for FCA by electrons, which has only indirect term, is much smaller than that for the holes. In all our calculations, we found, in agreement with literature, that the FCA coefficient, for both electrons and holes, is linearly dependent on the carrier density. Consequently σ is independent of the carrier density. The calculated σ is plotted as a function of wavelength for the four materials in Figure 6 for InAs and HgCdTe alloy. Note that the electron contribution is much smaller than the hole contribution as expected. The total cross section is small at shorter wavelengths because of the unavailability of holes at those energies in the HH band. Since the hole density is more near the zone center, the FCA cross section increases with the photon wavelength. However, because of the reduced intermixing of symmetries in both LH and HH band states near the zone center, the dipole matrix element decreases (and reaches zero at the center). Consequently, the cross section reduces with further increase in wavelength. This behavior is seen in all four materials considered here, but shown only for InAs and HgCdTe alloy in Figure 6.

When light energy is absorbed in semiconductors, equal densities of electrons and holes are created, which in turn release that energy to the lattice in the form of heat. To model light propagation through semiconductors, it is therefore necessary to know the FCA cross section as a function of both carrier concentration and temperature. The σ calculated for four materials as a function of wavelength and temperature are shown in Figure 7. In the literature, σ is usually assumed to be independent of temperature T. However, Figure 7 shows that σ varies strongly with T — at long wavelength σ decreases with T while at short wavelength it increases with T. This dependence can be explained using the second-order perturbation theory. The absorption coefficient is approximately the integrated product of the hole density and optical matrix element. Although this coefficient is divided by the total hole density to get σ, only a fraction of the holes participate in the absorption process because of energy and momentum conservation conditions. Even when the matrix elements do not change with T, the ratio of participating holes to the total number of holes has strong T dependence. For larger

photon energies (or shorter wavelengths), the VB states away from the zone center participate in absorption and the hole density in those states increase with T. For longer wavelength photon absorption, the holes near the zone center participate and the hole density decreases with T as the holes are thermally excited to higher energies. Consequently, the σ decreases with T.

We have calculated the T-dependence of σ in InAs and $Hg_{0.66}Cd_{0.34}Te$ at a wavelength of at 4.8 μm and in InSb and $Hg_{0.76}Cd_{0.24}Te$ at a wavelength of at 9.6 μm. Figure 8 shows that the σ at 9.6 μm decreases by a factor of 14 to 16 as the T is increased from 77K to 500K. σ at 4.8 μm in $Hg_{0.66}Cd_{0.34}Te$ is nearly a constant, but increases rapidly with T in InAs. It is important to note that T dependence of σ is in general very strong except at one or two wavelengths where the hole density does not change with T.

The wavelength dependent σ is calculated as a function of x in $Hg_{1-x}Cd_xTe$ alloys at T=300K and is shown in Figure 9. At smaller wavelengths, σ is independent of the x, as the participating hole population does not vary much with x. As x is increased, the spin-orbit coupling increases and the LH band bends more away from HH band.[35] Consequently, the energy conservation condition is satisfied in the BZ closer to zone center. The resulting increase in participating hole density causes σ to increase with x as seen in Figure 9.

Lifetimes

The carriers excited by the light absorption can participate in further absorption of light before they recombine. Hence the lifetimes τ of the excited electrons play a vital role in light propagation through the material. The full band structures and accurate scattering matrix elements are used in the lifetime calculations as described previously.[25,36,37] However, those calculations are now generalized to include the quasi Fermi levels for electrons and holes. The lifetimes limited by the Auger and radiative recombination are obtained as functions of temperature and carrier densities.

Parameter fit

Although the light propagation modeling studies,[3-6,22] including solutions to the rate equations,[22,24] use only a few parameters-- β, σ, τ, N ($=n_0+\Delta n$), T, and thickness d, the complication arises because of their interdependence. For example, β is a function of both N and T, but N depends on β and T. Similarly τ depends on T and N, which in turn depends on T. Eventually, β, σ and τ will determine the increase in T, which will in turn decide the values of those input parameters. Hence, for a self-consistent solution to the rate equations, it is preferable to have a closed functional form for the parameters β, σ and τ which is valid in the temperature and carrier density ranges of interest. The values of β and σ have been calculated at a wavelength of 4.8 μm in InAs and $Hg_{0.66}Cd_{0.34}Te$ and at 9.6 μm in InSb and $Hg_{0.76}Cd_{0.24}Te$, for 77K < T < 500K and 10^{14} $cm^{-3} < \Delta n < 10^{18}$ cm^{-3}. We have them fitted the values to the following expressions.

$$\beta = \frac{a}{1+\exp[(n-c)/b]}; \quad a = \sum_{i=0}^{4} a_i T^i \; ; \quad b = \sum_{i=0}^{4} b_i T^i; \quad c = \sum_{i=0}^{4} c_i T^i; \; n = (N \times 10^{-18}).$$

$$\sigma = \sum_{i=0}^{4} \sigma_i T^i$$

$$\log_{10}(\tau) = g + h \times \log_{10}(N); \quad g = \sum_{i=0}^{4} g_i T^i; \quad h = \sum_{i=0}^{4} h_i T^i$$

$$N_i = \sum_{i=0}^{4} p_i \left(\frac{1000}{T}\right)^i$$

The fitted parameters are given in Table 1 for four materials considered here. The table lists parameters only for AR lifetimes. We had previously calculated radiative recombination lifetimes and found them in general to be very long for these materials.[25] In addition, because of photon recycling present in thick samples studied here, the RR lifetimes are extremely long to have negligible effect on light propagation and hence the parameters are not listed here. The AR lifetimes in $Hg_{0.76}Cd_{0.24}Te$ are not calculated and not listed, as they are not expect to be substantially different from that in $Hg_{0.66}Cd_{0.34}Te$.

EXPERIMENTS AND RESULTS

In the approximation that the change in refractive index caused by photoexcited carriers in the material is negligible, the Helmholtz equation can be reduced to a simple

rate equation. A complete and self-consistent solution to these rate equations is needed to develop a detailed understanding of the mechanisms affecting the light propagation in the material. Recently we used above calculated parameters for InAs and solved the rate equations to explain the results obtained in our pump-probe experiment.[38] Since the details are published elsewhere,[38] only the results are discussed briefly here to provide continuity.

In the pump-probe experiment the charge carriers were generated by the pump using TPA. These carriers absorb the probe photos, resulting in very small probe transmission. As the carriers recombine, the probe transmission increases and reaches its incident value. The TPA used here ensures that the entire thickness of the sample is utilized for carrier generation at low incident irradiance. The 4.8 μm pump source was obtained by frequency doubling a TEA CO_2 laser to provide 128 ns (full-width at e^{-1} of the maximum) duration pulses with energies up to 10 mJ. The measurements are carried out at room temperature. First, we carried out a set of nonlinear absorption experiments with only the pump present. The measured transmitted intensity as a function of incident intensity and sample thickness is shown in Figure 10. As the intensity is increased, more carriers are generated and the absorption increases, resulting in a decreased transmission. Similarly, as the thickness is increased, light is absorbed more. These trends are clearly observed. Also in Figure 10, we have plotted the calculated transmitted intensity obtained from solving the rate equations with the values given in Table 1. In addition to the Auger recombination, we have included lifetimes limited by Shockley-Read-Hall (SRH) mechanism. The SRH scattering is not intrinsic to the material and depends on external variables such as the growth temperature and pressure. Our detailed calculations carried out previously[39] indicate a nearly T-independent SRH lifetime of 200 ns in a 2×10^{16} cm^{-3} n-doped InAs. Although the InAs sample studied here is only 10^{15} cm^{-3} n-doped, the excess carriers generated by the pump is of the order of $1\text{-}2 \times 10^{16}$ cm^{-3}, and justifies the use of the above calculated SRH lifetimes. We further assumed that SRH lifetime decreases linearly with excess carrier density. We see that calculated transmission intensity agrees very well with measured values for all thicknesses studied. The calculations are then extended to understand the pump-probe results shown in Figure 11. With only the SRH values used in an approximation, we see that the time-dependent

transmitted probe intensity calculated for the three input energies explain the observed variation very well.

CONCLUSIONS

We have used a full bandstructure, obtained from a hybrid pseudopotential tight-binding Hamiltonian, to calculate the temperature and carrier density dependent two photon absorption coefficients, free carrier absorption cross section, and Auger lifetimes in InAs, InSb and HgCdTe alloys. Accuracy of the calculations are enhanced with use of the quasi Fermi levels, intrinsic carrier densities, detailed optical and scattering matrix elements, and complete integration over the entire BZ. The calculated parameters are fitted to closed-form functions and used in the rate equations to obtain the transmitted intensity as a function of time, incident intensity, and sample thickness. The transmission spectra calculated, with only SRH lifetimes as a parameter, agree very well the measured values. We showed that with accurate evaluation of all parameters, the modeling can provide a detailed guidance in understanding the underlying mechanisms and in choosing materials for light propagation applications. The closed-form expressions for the fundamental parameters given here can be used in other accurate light propagation models.

Acknowledgements

SK and ZY gratefully acknowledge the funding from WPAFB contract F33615-97-D-5403 through Anteon Corporation.

REFERENCES

[1] L.W. Tutt and T.F. Boggess, Prog. Q. Electron. **17**, 299 (1993).

[2] E. Garmire, IEEE J. on Selected Topics in Q. Elec. **6**, 1094 (2000).

[3] D.L. Kovsh, S. Yang, D.J. Hagan, E. Van Stryland, Nonlinear Optical Liquids for Power Limiting and Imaging, C.M. Lawson, ed., SPIE **3472**, 163 (1988); Appl. Opt. **38**, 5168 (1999).

[4] J. Robertson, P. Milsom, J. Duignan, and G. Bourhill, Opt. Lett. **25**, 1258 (2000).

[5] J. Robertson, A. Smith, J. Duignan, P. Milsom, and G. Bourhil, Appl. Phys. Lett. **78**, 1183 (2001).

[6] E. Van Stryland, Y.Y. Wu, D.J. Hagan, M.J. Soileau, and K. Mansour, J. Opt. Soc. Am. **5**, 1980 (1988).

[7] R.M. Grant, J. Opt. Soc. Am. **55**, 1457 (1965).

[8] R.M. Culpepper and J.R. Dixon, J. Opt. Soc. Am. **58**, 96 (1968).

[9] A. Miller, A. Johnson, J. Dempsey, J. Smith, C.R. Pidgeon, and G.D. Holah, J. Phys. C **12**, 4839 (1979).

[10] A.M. Johnson, C.R. Pidgeon, and J. Dempsey, Phys. Rev. B **22,** 825 (1980).

[11] M.H. Weiler, Solid State Comm. **39**, 937 (1981).

[12] B.S. Wherrett, J. Opt. Soc. Am. B **1**, 67 (1984).

[14] E. Van Stryland, M.A. Woodall, H. Vanherzeele, and M.J. Soileau, Opt. Lett. **10**, 490 (1985).

[15] M.S. Bahaei, P. Mukherjee, and H.S. Kwok, Opt. Soc. Am. B **3,** 379 (1986); and references cited there in.

[16] E. Van Stryland, H. Vanherzeele, M.A. Woodall, M.J. Soileau, A.L. Smirl, S. Guha, and T. Boggese, Opt. Engg. **24**, 613 (1985).

[17] D.C. Hutchings and E. Van Stryland, J. Opt. Soc. Am. B **9**, 2065 (1992).

[18] B.N. Murdin, C.R. Pidgeon, A.K. Kar, D.A. aroszynski, J.-M.Ortega, R.Prazeres, and F. Glotin, Opt. Mater. **2**, 89 (1993).

[19] B.N. Murdin, C. Mervielle, A.K. Kar, C.R. Pidgeon, D.A. Jaroszynski, J.-M. Ortega, R. Prazeres, and F. Glotin, Opt. Mater. (1993).

[20] K.W. Berryman and C.W. Rella, Phys. Rev. B{\bf 55}, 7148 (1997).

[21] M.B. Haeri, S.R. Kingham, and P. Milsom, J. Appl. Phys. {\bf 99}, 13514 (2006).

[22] S. Krishnamurthy, A. Sher, and A.-B. Chen, J. Appl. Phys. **88**, 260 (2000).

[23] S. Krishnamurthy, K. Nashold, and A. Sher, Appl. Phys. Lett., **77**, 355 (2000).

[24] A. Kobyakov, D.J. Hogen, and E.W. Van Stryland, J. Opt. Soc. Am. B **17**, 1884 (2000).

[25] S. Krishnamurthy, M.A. Berding, Z. Yu, J. Elec. Mater. **35**, 1369 (2006).

[26] A.-B. Chen and A. Sher, *Semiconductor alloys* (New York, Plenum 1985)

[27] S. Krishnamurthy, A. Sher, and A.-B. Chen, J. Elec. Mater. **24**, 1121 (1995).

[28] G.L. Hansen, J.L. Schmit, and T.N. Casselman, J. Appl. Phys. **53**, 7099 (1982).

[29] Z. Fang, K. Y. Ma, D. H. Jaw, R. M. Cohen, and G. B. Stringfellow, *J. Appl. Phys.* **67**, 7034 (1990).

[30] C.L. Littler, D. G. Seller, *Appl. Phys. Lett.* **46**, 986 (1985).

[31] S. M. Sze, *Physics of Semiconductor Devices* (New York; John Wiley & Sons, 1981), p. 23.

[32] J.R. Meyer, C.A Hoffman, F.J. Bartoli D.A. Arnold, S. Sivananthan and J. P. Faurie, Semicond, Sci. Technol. **8**, 805 (1993).

[33] I. Vurgaftman, J.R. Meyer, C.A. Hoffman, D. Redfern, J. Antoszewski, L. Faraone, and J.R. Lindemuth, J. Appl. Phys. **84**, 4966 (1998).

[34] C. H. Swartz, R. P. Tompkins, N. C. Giles, T. H. Myers, D. D. Edwall, J. Ellsworth, E. Piquette, J. Arias, M. Berding, S. Krishnamurthy, I. Vurgaftman, and J. R. Meyer, J. Electron. Mater. **36**, 728 (2004).

[35] Z.G. Yu, S. Krishnamurthy, and S. Guha, J. Opt. Soc. Am. B **23**, xxxx (2006)

[36] S. Krishnamurthy, A. Sher, and A.-B. Chen, J. Appl. Phys. **82**, 5540 (1997).

[37] S. Krishnamurthy and T. Casselman, J. Elec. Mater.. **28**, 828 (2000)

[38] S. Krishnamurthy, Z.G. Yu, S. Guha, and L. Gonzalez, Appl. Phys. Lett. [Accepted, Oct. 16, 2006].

[39] S. Krishnamurthy and M.A. Berding, J. Appl. Phys. **90**, 848 (2001).

TABLE 1

Parameters	InAs	$Hg_{0.66}Cd_{0.34}Te$	InSb	$Hg_{0.76}Cd_{0.44}Te$
a_0	0.20516	2.1620	2.5913	48.074
a_1	0.0015299	-0.00394730	0.0039691	-0.45516
a_2	-1.859×10^{-6}	1.3372×10^{-5}	0.00012589	0.0029993
a_3	1.8466×10^{-9}	-3.1219×10^{-8}	-4.6698×10^{-7}	-8.3954×10^{-6}
a_4	3.4373×10^{-12}	3.3459×10^{-11}	6.6038×10^{-10}	7.718×10^{-9}
b_0	-0.034375	0.11742	-0.0019728	0.3932
b_1	0.0020645	0.00041377	0.00031268	-0.0033771
b_2	-2.1108×10^{-6}	5.3520×10^{-6}	5.2291×10^{-7}	2.0397×10^{-5}
b_3	-6.5561×10^{-10}	-6.6517×10^{-9}	7.3333×10^{-10}	-5.051×10^{-8}
b_4	5.6352×10^{-12}	5.4334×10^{-12}	3.0668×10^{-12}	4.563×10^{-11}
c_0	0.45859	1.2756	-0.04522	0.21089
c_1	-0.0013534	-0.00095861	0.0	0.0032988
c_2	1.0666×10^{-5}	1.0237×10^{-5}	0.0	-3.8836×10^{-5}
c_3	-1.1906×10^{-8}	-1.8417×10^{-8}	0.0	1.1845×10^{-7}
c_4	4.3216×10^{-12}	-7.1237×10^{-12}	0.0	-1.1285×10^{-10}
σ_0	-2.8164	-0.95501	46.1	65.296
σ_1	0.044098	0.16677	-0.2929	-0.57162
σ_2	5.9962e-06	-0.00081382	0.00082667	0.0021109
σ_3	-2.2463e-07	1.4824×10^{-6}	-1.1092×10^{-6}	-3.4952×10^{-6}
σ_4	2.3863e-10	-9.422×10^{-10}	5.6047×10^{-10}	2.1284×10^{-9}
g_0	40.467	43.429	47.74	43.429
g_1	-0.02737	-0.06712	-0.15205	-0.06712
g_2	-8.597×10^{-6}	2.480×10^{-4}	0.0007528	2.480×10^{-4}
g_3	2.2386×10^{-7}	-3.7801×10^{-7}	-1.6296×10^{-6}	-3.7801×10^{-7}
g_4	-3.122×10^{-10}	1.8071×10^{-10}	1.241×10^{-9}	1.8071×10^{-10}
h_0	14.336	15.1230	14.26	15.1230
h_1	0.037678	0.034190	0.038101	0.034190
h_2	-0.00011995	-1.1134×10^{-4}	-0.00010939	-1.1134×10^{-4}
h_3	1.8793e-07	1.8605×10^{-7}	1.4327×10^{-7}	1.8605×10^{-7}
h_4	-1.152e-10	-1.2588×10^{-10}	-6.6935×10^{-11}	-1.2588×10^{-10}
p_0	9.2435	11.534	8.5016	8.7934
p_1	-2.7345	-3.9967	-1.7296	-2.1725
p_2	0.0	0.0	0.0	0.19217
p_3	0.0	0.0	0.0	-0.013391
p_4	0.0	0.0	0.0	0.00036021

Figure Captions:

Figure 1. Variation of energy gap (dashed line) and intrinsic Fermi energy (dotted line) with temperature. Also shown are electron quasi Fermi energy (thin solid line), hole quasi Fermi energy (thick solid line) for various photoexcited carrier densities ($\Delta n=\Delta p$).

Figure 2. Variation of intrinsic carrier density with temperature

Figure 3. Two photon absorption coefficient as a function of wavelength and temperature.

Figure 4. Two photon absorption coefficient as a function of excited carrier density at (a) at 300K and (b) 77K.

Figure 5. Two photon absorption coefficient as a function of wavelength in HgCdTe alloys at 300K.

Figure 6. Wavelength-dependent free carrier absorption cross section at 300K

Figure 7. Wavelength-dependent free carrier absorption cross section at 77K and 300K.

Figure 8. Temperature-dependent free carrier absorption at 4.8 μm in InAs and $Hg_{0.66}Cd_{0.34}Te$ and at 9.6 μm in InSb and $Hg_{0.76}Cd_{0.24}Te$ at 300K.

Figure 9. Wavelength-dependent free carrier absorption cross section as a function of Cd concentration in HgCdTe alloys at 300K.

Figure 10. Comparison of normalized pump transmission coefficient measured (data) at 300K in 10^{15} n-doped InAs with that calculated (solid lines) for four thicknesses.

Figure 11. Comparison of normalized probe transmission coefficient measured (data) at 300K in 10^{15} n-doped InAs with that calculated (solid lines) for three beam energies.

Figure 1 Krishnamurthy et al.

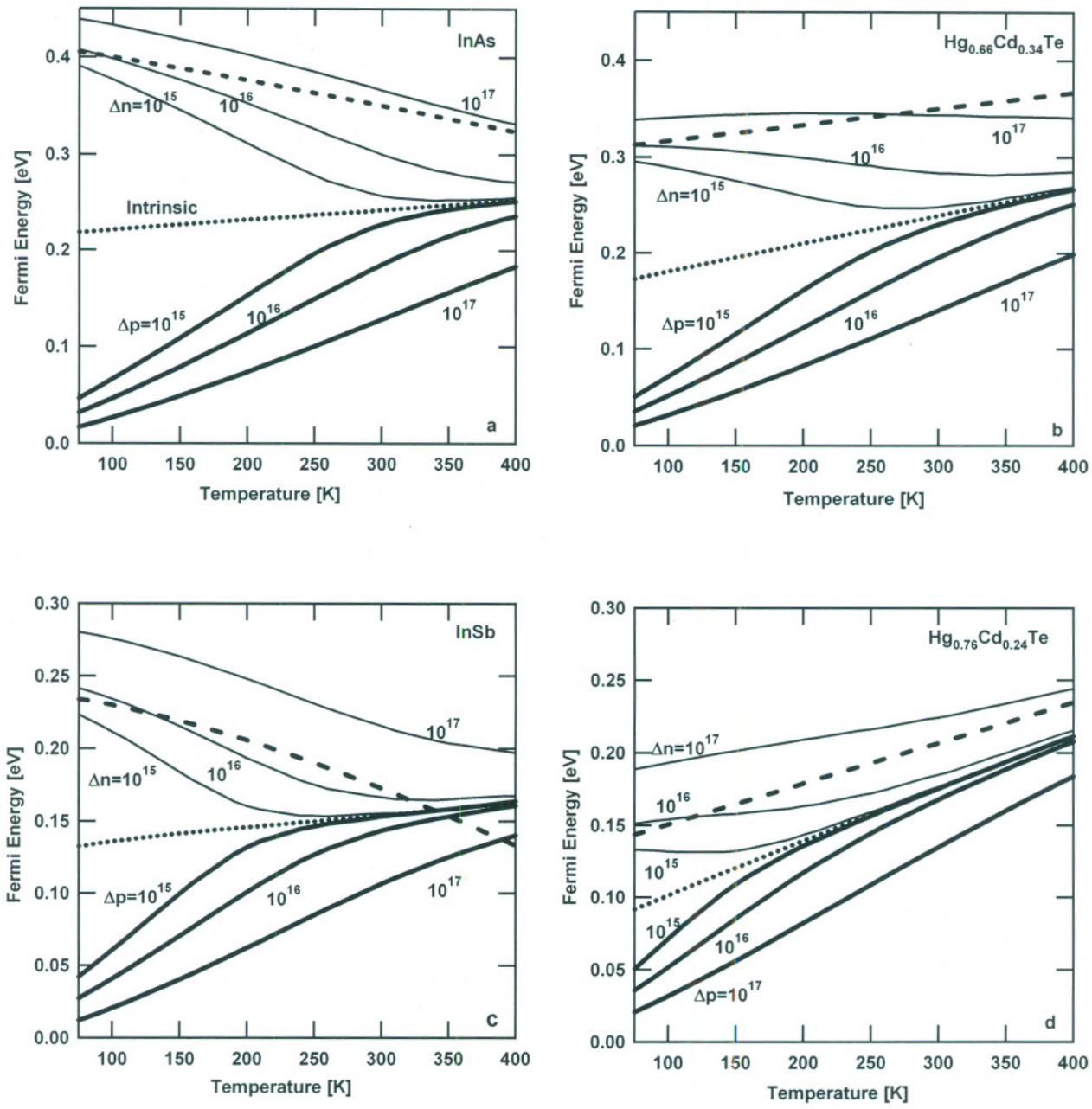

Figure 2 Krishnamurthy et al.

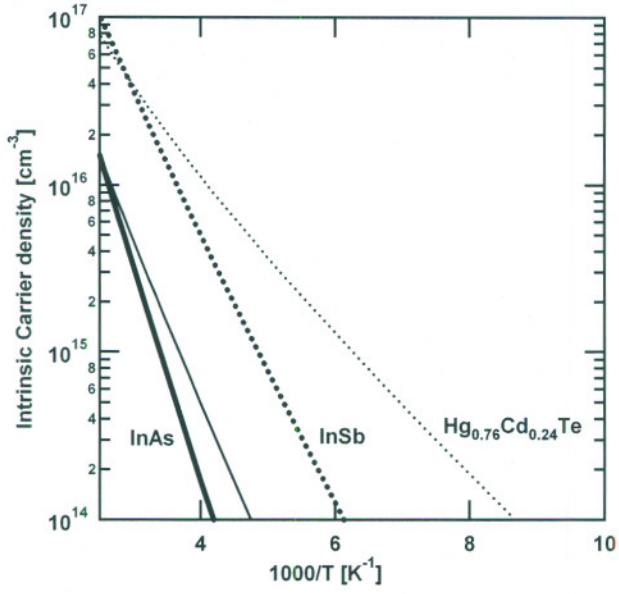

Figure 3 Krishnamurthy et al.

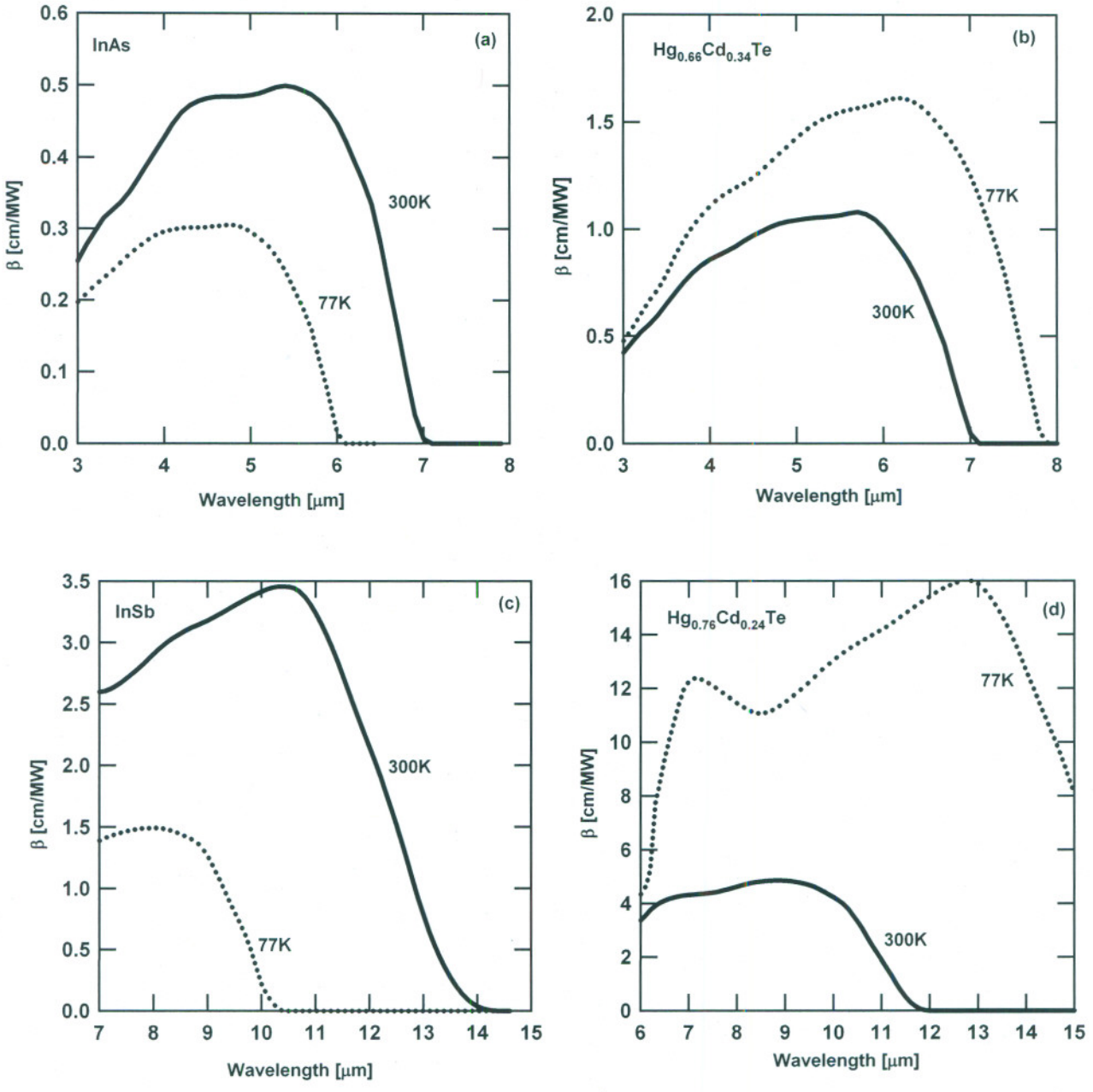

Figure 4 Krishnamurthy et al.

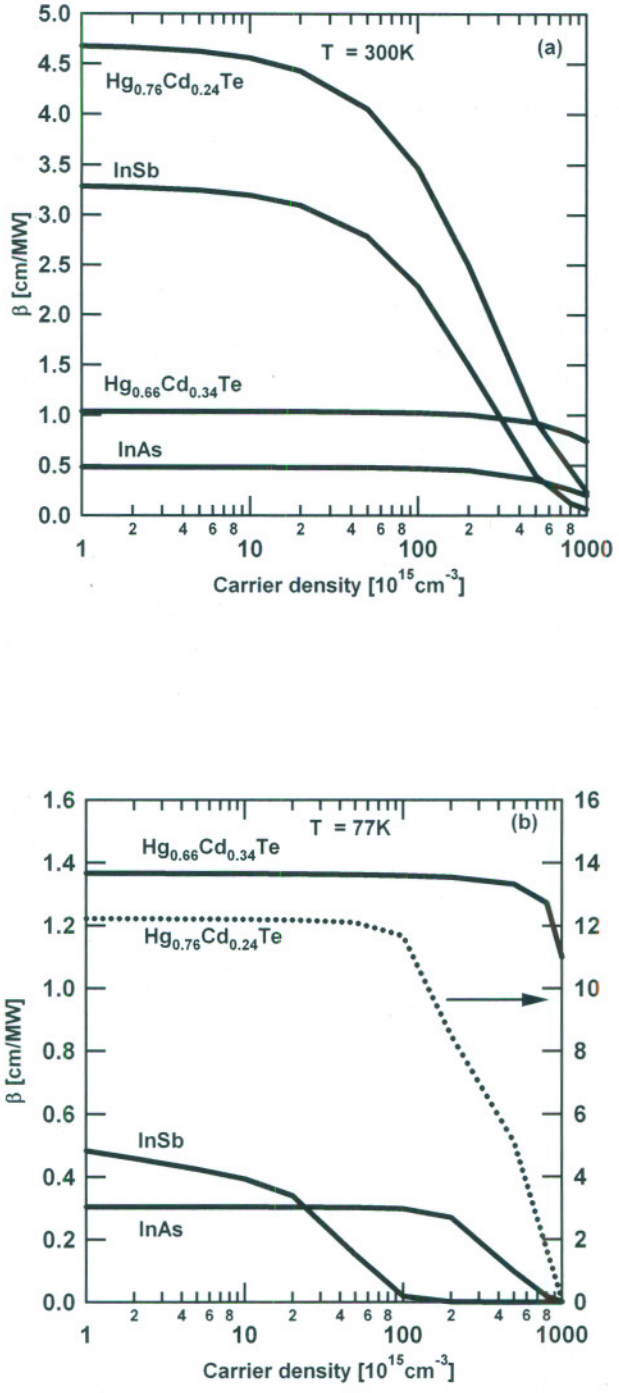

Figure 5 Krishnamurthy et al.

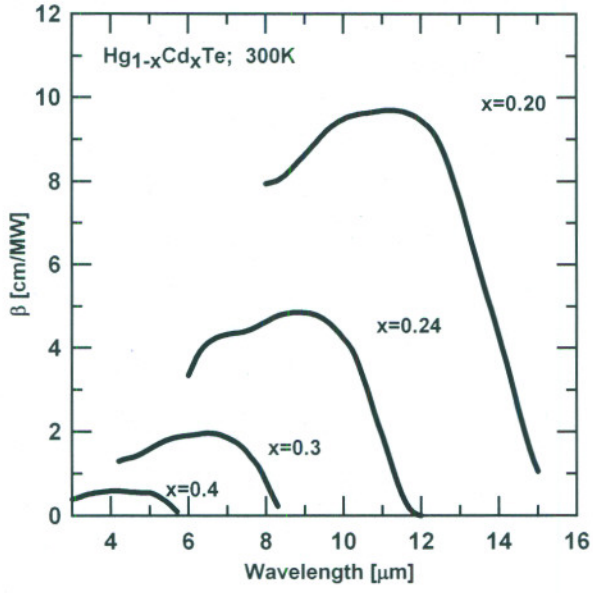

Figure 6 Krishnamurthy et al.

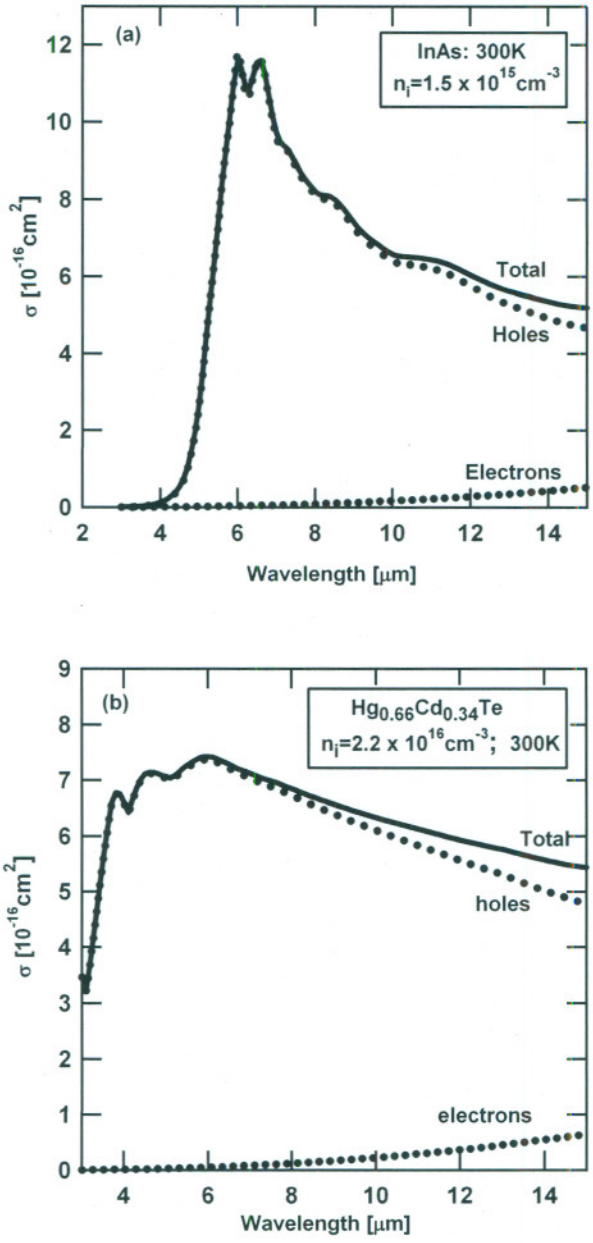

Figure 7 Krishnamurthy et al.

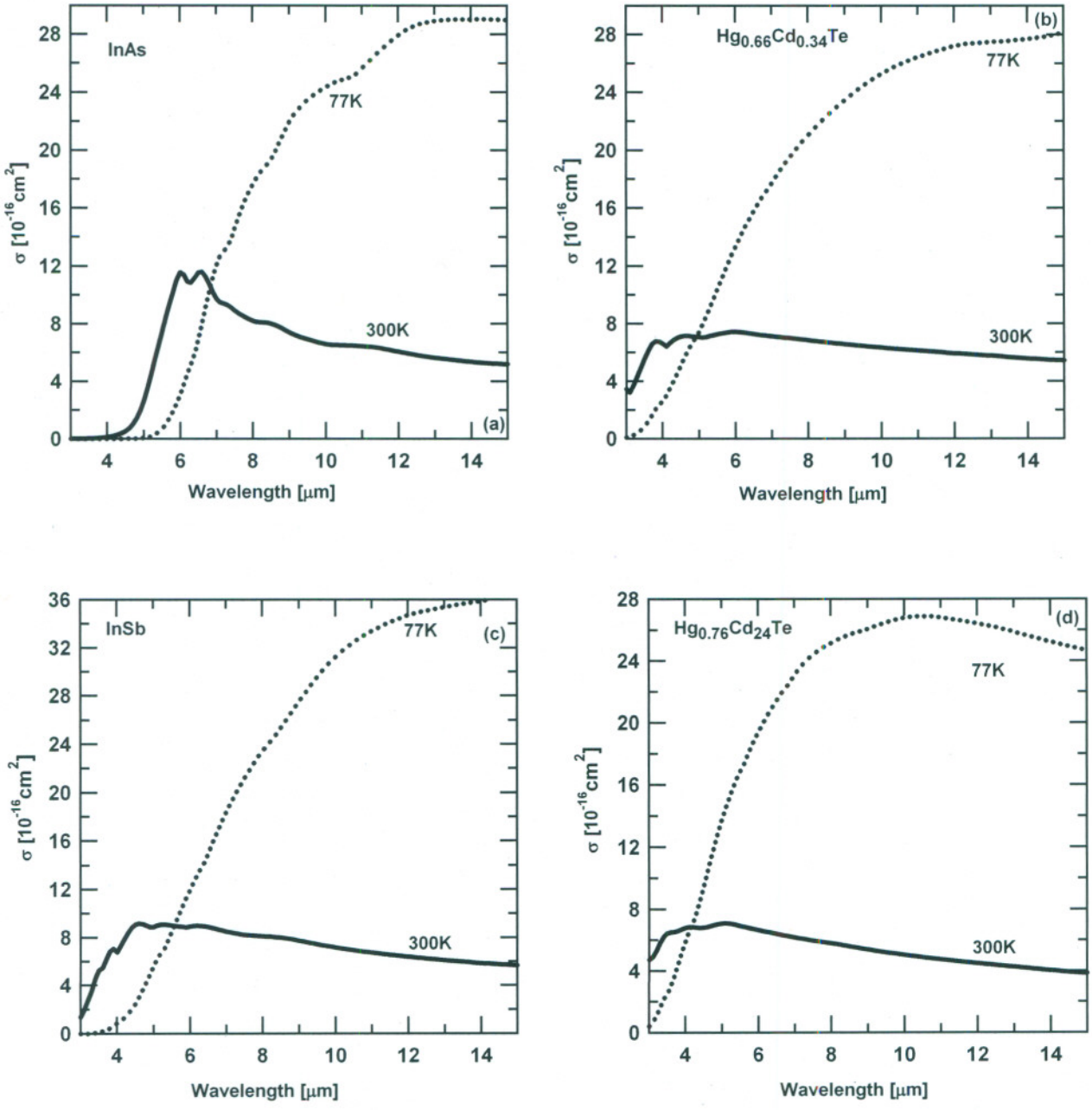

Figure 8 Krishnamurthy et al.

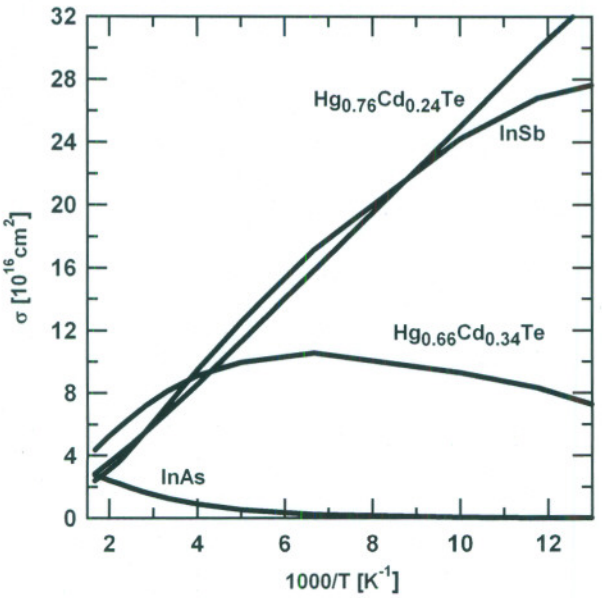

Figure 9 Krishnamurthy et al.

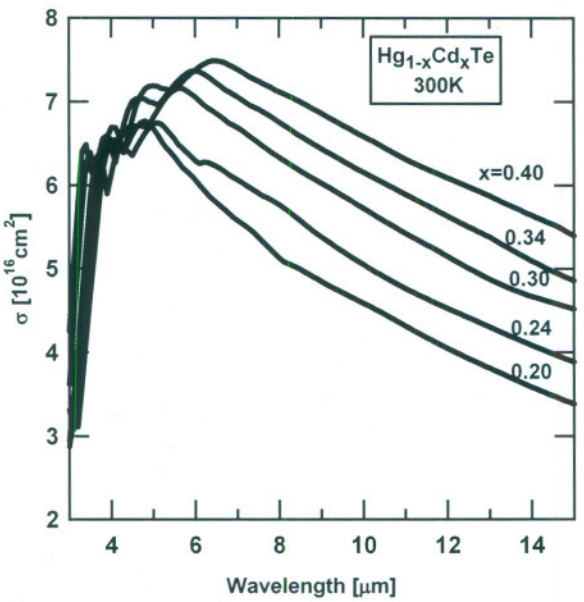

Figure 10 Krishnamurthy et al.

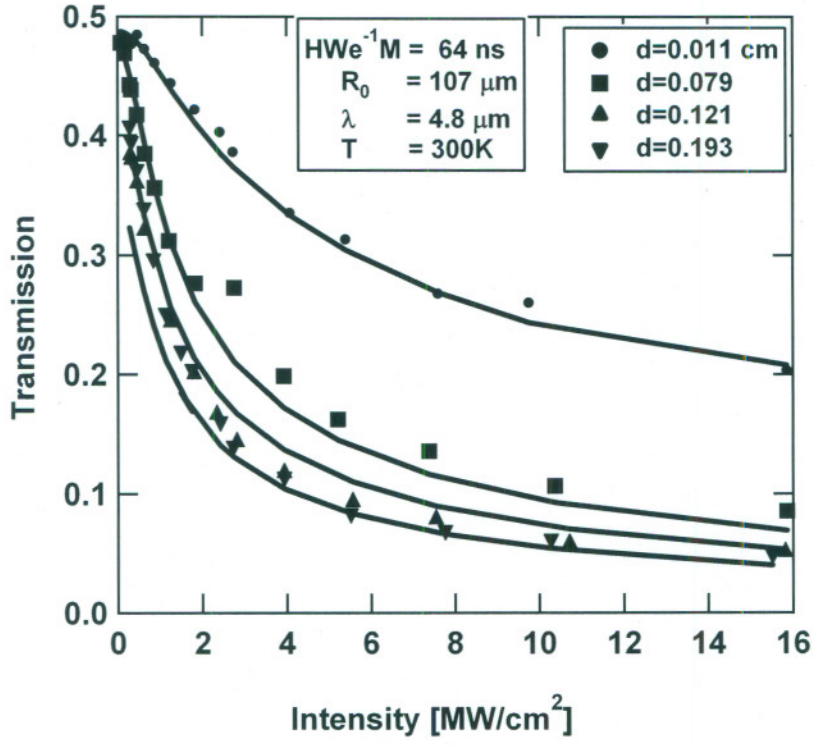

Figure 11 Krishnamurthy et al.